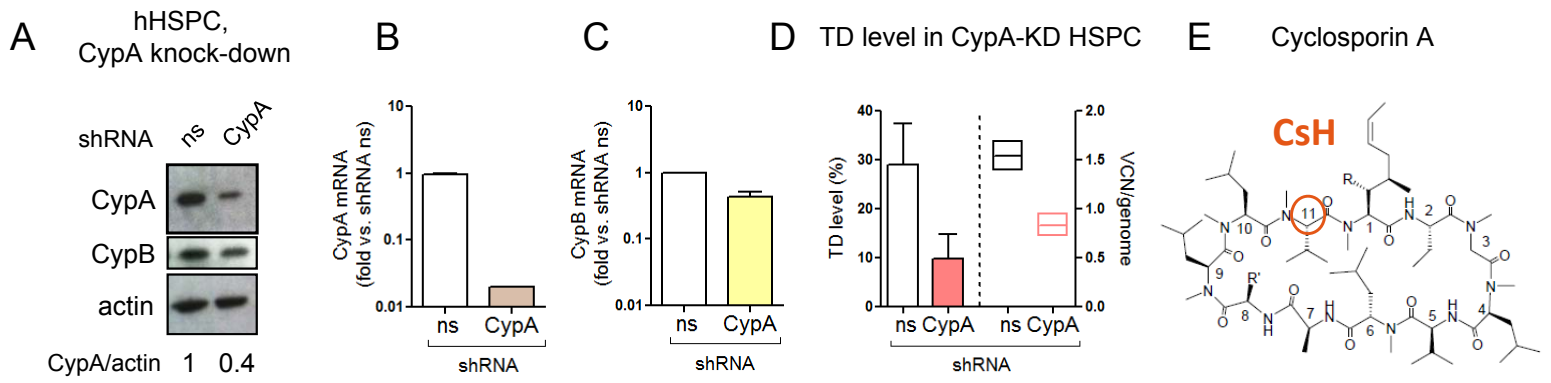


**Cell Stem Cell, Volume 23**

**Supplemental Information**

**Cyclosporine H Overcomes Innate Immune  
Restrictions to Improve Lentiviral Transduction  
and Gene Editing In Human Hematopoietic Stem Cells**

**Carolina Petrillo, Lucy G. Thorne, Giulia Unali, Giulia Schioli, Anna M.S. Giordano, Francesco Piras, Ivan Cuccovillo, Sarah J. Petit, Fatima Ahsan, Mahdad Noursadeghi, Simon Clare, Pietro Genovese, Bernhard Gentner, Luigi Naldini, Greg J. Towers, and Anna Kajaste-Rudnitski**



Name	Modification	Functions
CsA	-	Immunosuppressive and CypA inhibition
CsH	Residue 11 (D-MeVal)	Non immunosuppressive; no CypA inhibition; binds FPR-1

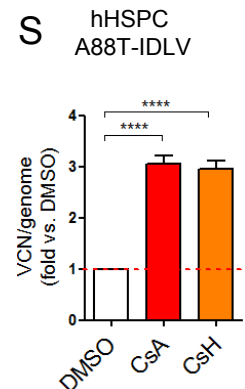
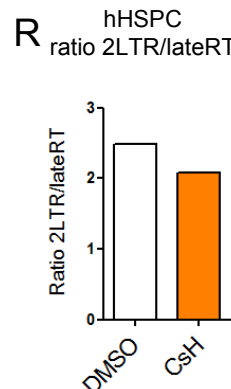
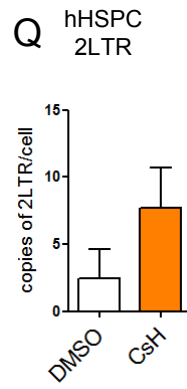
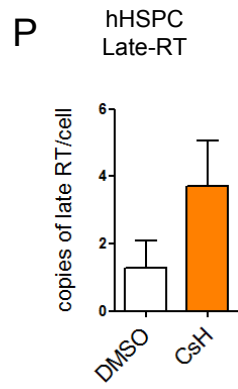
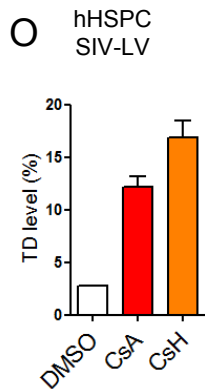
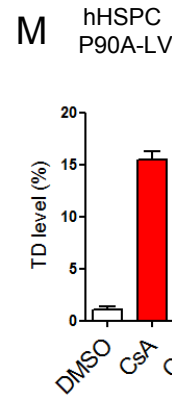
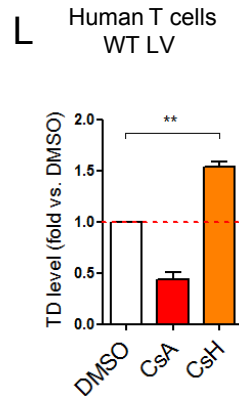
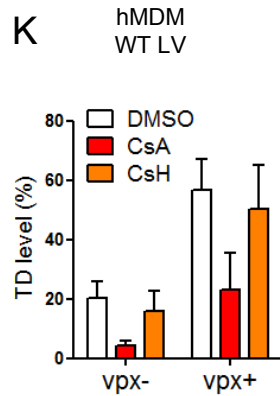
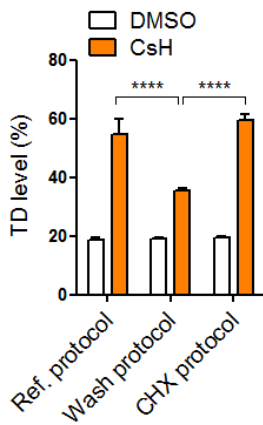
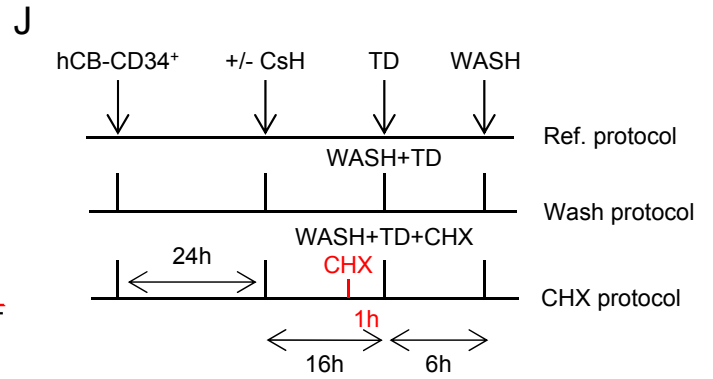
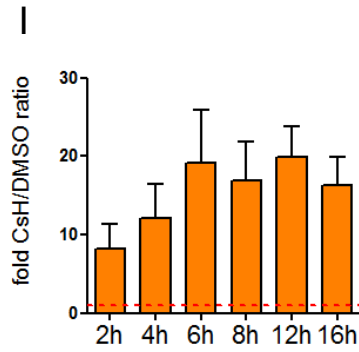
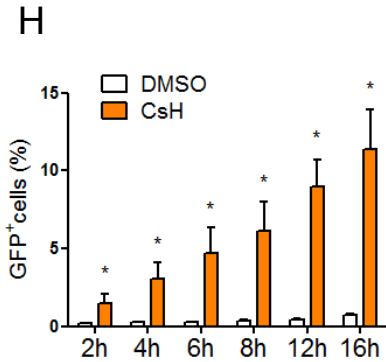
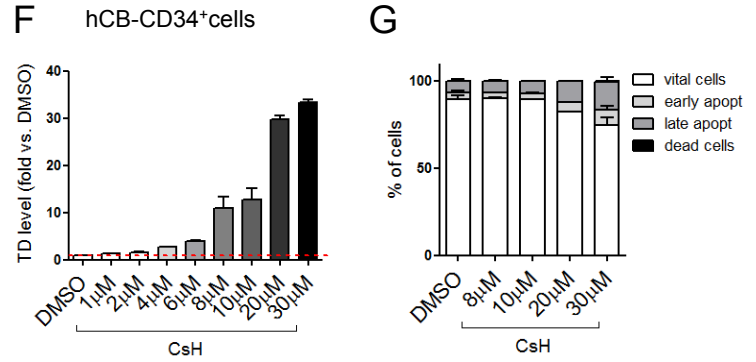


**Figure S1. CsH is a more potent transduction enhancer than CsA, Related to Figure 1.**

**(A-C)** Human CB-derived CD34<sup>+</sup> cells were transduced with an LV expressing a shRNA against CypA or a non-silencing control at an MOI of 100 and knock-down (KD) of CypA was verified by Western Blot **(A)** and by mRNA expression **(B)**. **(A, C)** Levels of CypB were monitored as a control of RNAi specificity.

**(D)** Impact of the depletion was then evaluated by transducing the cells with a second LV at an MOI of 10 and evaluating transduction efficiency by FACS in terms of GFP<sup>+</sup> cells and by VCN.

**(E)** Cyclosporins chemical structures and properties. FPR-1 stands for formyl peptide receptor 1.

**(F)** Transduction efficiency was evaluated in human CB-CD34<sup>+</sup> cells in presence or absence of different concentrations of CsH (mean ± SEM, n=2).

**(G)** Apoptosis analysis was performed in human CB-CD34<sup>+</sup> cells in presence or absence of different CsH concentrations (mean ± SEM, n=2).

**(H, I)** Human CB-CD34<sup>+</sup> cells were exposed for different time to PGK-GFP LV MOI=1 in presence or absence of 8 μM CsH. Transduction efficiency was evaluated 5 days after TD at FACS and expressed as % of GFP<sup>+</sup> cells in H or as fold increase of CsH/DMSO control in I (mean ± SEM, n=4, Mann Whitney test, \*p≤0.05).

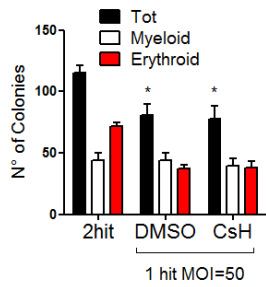
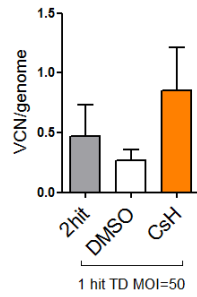
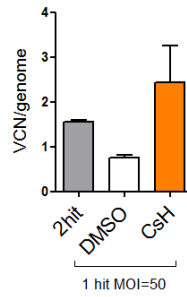
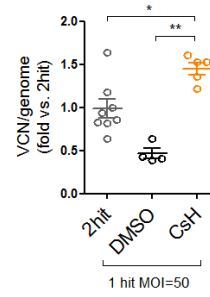
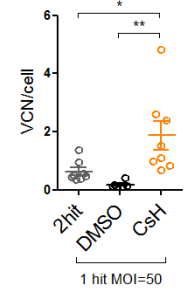
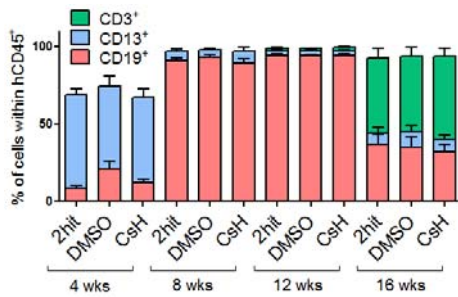
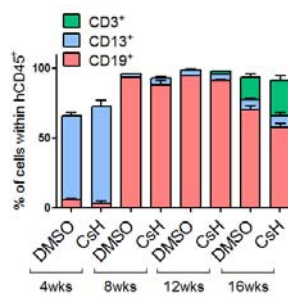
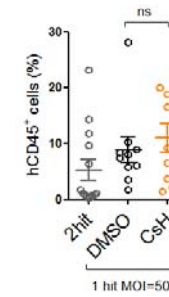
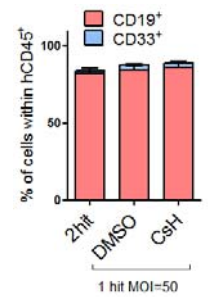
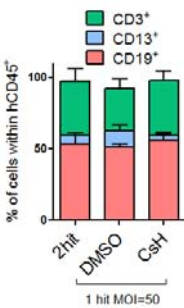
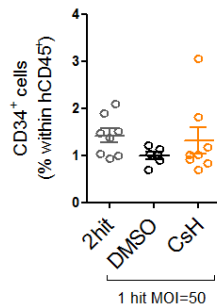
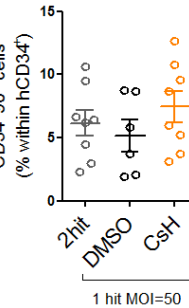
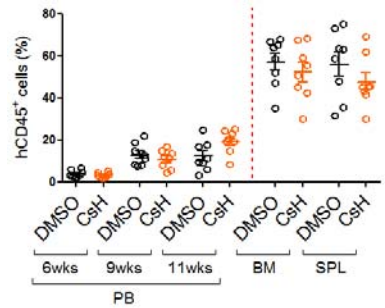
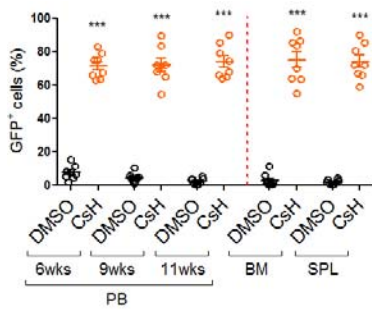
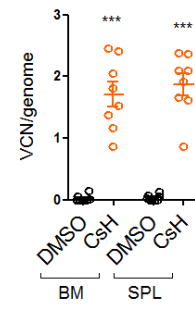
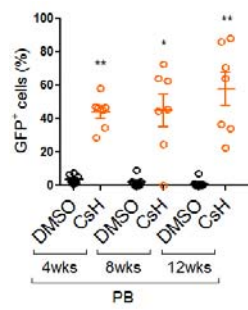
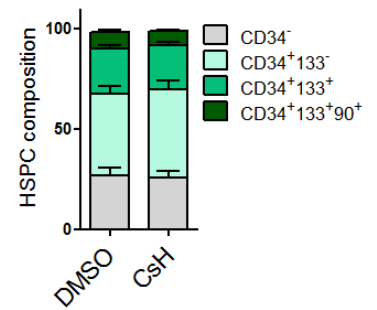
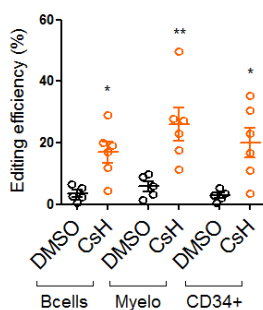
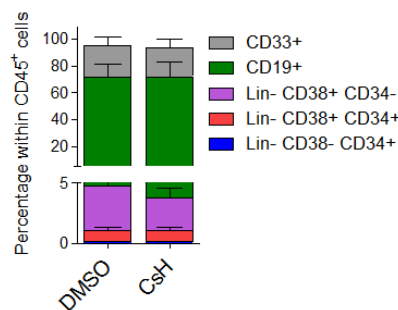
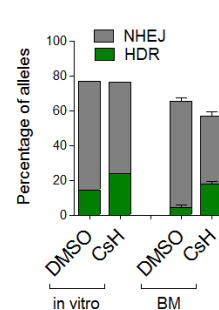
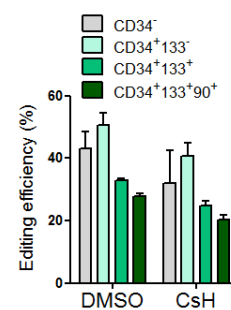
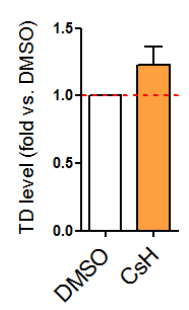
**(J)** Human CB-CD34<sup>+</sup> cells were transduced for 6 hours using different protocols +/- CsH and TD levels were evaluated by FACS (mean ± SEM, n=4, One way ANOVA with Bonferroni's multiple comparison, \*\*\*\*p≤0.0001).

**(K)** Human monocyte-derived macrophages (MDM) pre-exposed or not to Vpx (mean ± SEM, n=3) and **(L)** primary CD3<sup>+</sup> or CD4<sup>+</sup> T cells were transduced at an MOI of 1 in presence or absence of 8 μM CsA/H (mean ± SEM, n=8, Wilcoxon Signed Rank Test vs. DMSO=1, \*\*p=0.0078).

**(M-O)** Human CD34<sup>+</sup> cells from different sources were transduced with different LV vectors as indicated, in presence or absence of 8 μM CsA/H. Transduction efficiencies were evaluated 5 days post-transduction (mean ± SEM, n=2).

**(P-R)** Late-RT and 2LTR circle replication intermediates were measured in CB-CD34<sup>+</sup> cells transduced with an LV MOI 100 at 6 or 24 hours post-transduction, respectively. LateRT and 2LTR products were expressed as copies/cell in P and Q, as the ratio between 2LTR/lateRT copies in R (mean ± SEM, n≥3).

**(S)** Human CD34<sup>+</sup> cells from different sources were transduced with different A88T capsid mutant IDLV, in presence or absence of 8 μM CsA/H. Transduction efficiencies were evaluated 5 days post-transduction and expressed as fold increase vs. DMSO control (mean ± SEM, n=4, One way ANOVA with Bonferroni's multiple comparison, \*\*\*\*p≤0.0001).

**A** CFU count**B** VCN LC**C** VCN CFU**D** VCN PB**E** VCN SPL**F** PB lineage composition**G** PB lineage composition**H** SPL of mice**I** BM of mice**J** SPL of mice**K** BM of mice**L** BM of mice**M** Primary NSG mice**N****O****P** II NSG mice**Q** GE IDLV**R****S****T****U** GE AAV6**V** hHSPC AAV6

**Figure S2. CsH increases LV transduction and gene editing efficiencies in SCID-repopulating HSPC, Related to Figure 2.** Human mPB-derived CD34<sup>+</sup> cells were transduced with a clinical-grade LV comparing different transduction protocols as reported in Fig.2A.

**(A)** The number of myeloid and erythroid colony-forming units (CFU) were assessed *in vitro* two weeks after plating (mean ± SEM; n=8; Dunn's adjusted Kruskal–Wallis test vs. 2hit total CFU, \*p≤0.05).

VCN/genome were measured in **(B)** liquid culture (LC) and **(C)** bulk CFU 14 days post-transduction (mean ± SEM, n=2).

**(D)** VCN/genome were measured in the peripheral blood (PB) of NSG-mice 8 weeks after transplantation (mean ± SEM, n≥4, One way ANOVA with Bonferroni's multiple comparison, \*p≤0.05, \*\*p ≤0.01) and **(E)** in the spleen (SPL) 18 weeks post-transplant (mean ± SEM, n≥6; One way ANOVA with Bonferroni's multiple comparison, ns=not significant, \*p≤0.05, \*\*p ≤0.01).

Percentages of human B, myeloid and lymphoid cell lineages (hCD19<sup>+</sup>, hCD33<sup>+</sup> and hCD3<sup>+</sup> respectively) within human CD45<sup>+</sup> cells are shown in the **(F, G)** PB over-time, **(I)** bone marrow (BM) and **(J)** spleen of mice at 18 weeks.

**(H)** Engraftment levels of human CD45<sup>+</sup> cells in the SPL were shown at 18 weeks post-transplant (mean ± SEM; n≥11; Dunn's adjusted Kruskal–Wallis, ns=not significant).

**(K, L)** Percentages of CD34<sup>+</sup> within human CD45<sup>+</sup> cells and CD34<sup>+</sup>90<sup>+</sup> within CD34<sup>+</sup> cells were measured in the BM of mice 18 weeks post-transplantation.

Human CB-CD34<sup>+</sup> cells were transduced with a purified PGK-GFP LV at MOI=20 as in Fig. 2F. **(M)** Engraftment and **(N)** transduction levels were shown in the PB over-time as well as in the BM and SPL of primary mice 12 weeks after transplantation.

**(O)** VCN/human genome were also measured in the BM and in the SPL of mice (mean ± SEM; n= 8 mice per group, Mann-Whitney test versus DMSO control, \*\*\*p≤0.001).

**(P)** GFP<sup>+</sup> cells were measured in the PB of secondary mice at different times post-transplantation.

**(Q)** Subpopulation composition of treated human CB-CD34<sup>+</sup> cells from Fig.2J measured by flow cytometry 3 days after electroporation (n=7).

**(R)** Editing efficiency measured by ddPCR in sorted CD34<sup>+</sup> HSPCs, CD19<sup>+</sup> B cells, and CD33<sup>+</sup> myeloid cells from the BM of mice in Fig. 2M 19 weeks post-transplantation (Mann-Whitney Test).

**(S)** Percentage of the indicated subpopulations measured within grafted human cells in the BM of mice from Fig. 2M.

**(T)** Percentages of NHEJ and HDR were measured *in vitro* and in the BM of mice at sacrifice from Fig. 2J-2M.

**(U)** Percentage of edited cells using AAV6 as donor template was measured within the indicated subpopulations 3 days after editing.

**(V)** hCB-CD34<sup>+</sup> cells were transduced with an Adeno-associated vector type 6 (AAV6) MOI=10000 in presence or absence of 8μM CsH and TD levels were evaluated by FACS and expressed as fold increase CsH versus DMSO control.

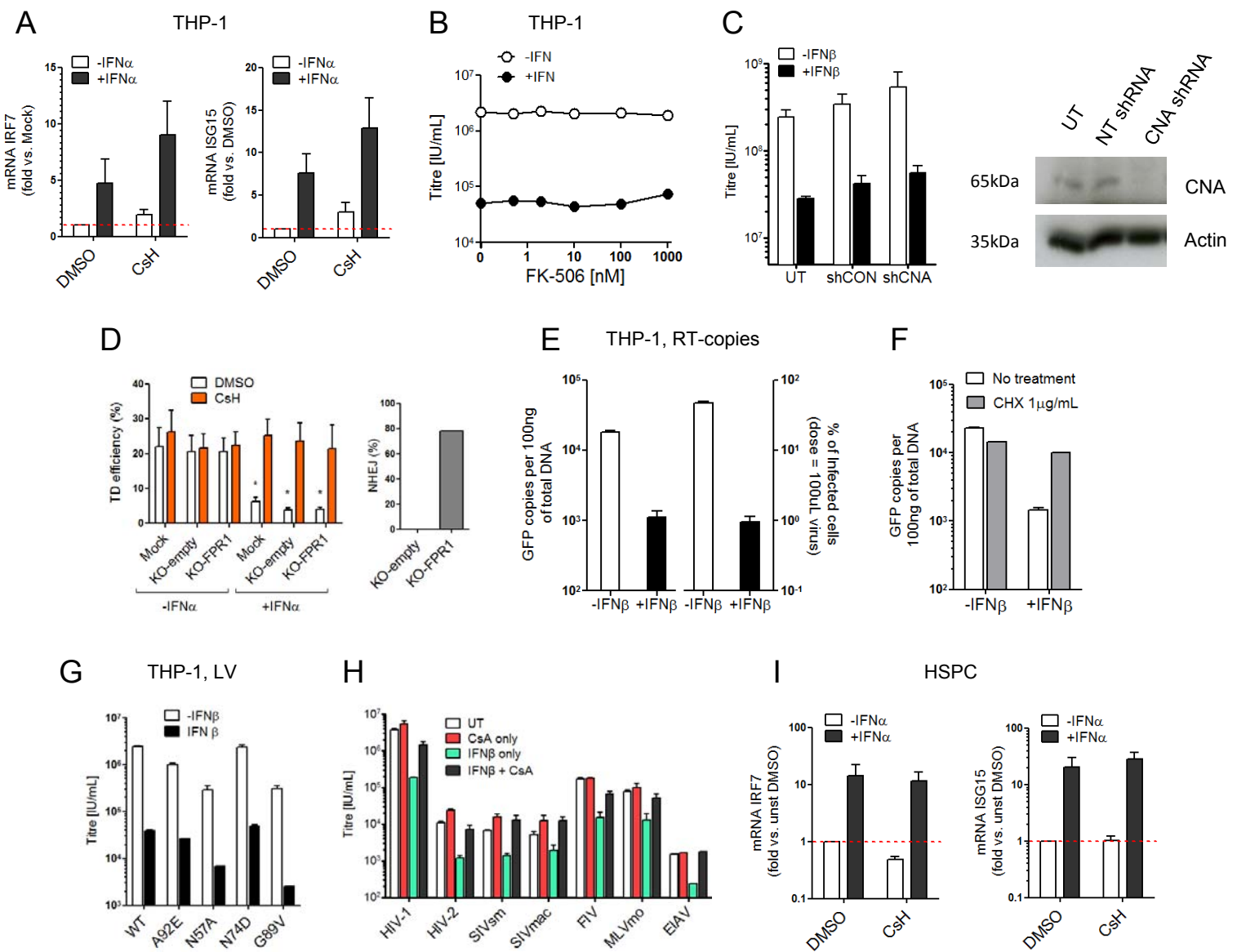


**Figure S3. Cyclosporin counteracts an IFN-induced lentiviral restriction in THP-1 and HSPC, Related to Figure 3.**

**(A)** THP-1 were pre-stimulated with 1000 IU/mL of human IFN $\alpha$  for 24 hours followed by 16 hours of exposure or not to 8 $\mu$ M CsH. Upregulation of selected IFN-stimulated genes (ISG) was assessed by RT-qPCR (mean  $\pm$  SEM, n=3).

**(B)** FK-506 does not rescue type I IFN-induced restriction of transduction as measured by directly titrating the vector on THP-1 cells in presence of different FK-506 concentrations.

**(C)** Calcineurin was depleted in THP-1 cells prior to treatment with 1ng/ml human IFN $\beta$  for 24 h and evaluation of transduction efficiency by titration of LV.

**(D)** THP-1 cells deleted for FPR1, as measured by % of non-homologous end-joining (NHEJ), were transduced with an LV at MOI 1 +/- 8 $\mu$ M CsH. Transduction efficiencies were assessed by FACS 5 days post second transduction (mean  $\pm$  SEM, n=4, Mann Whitney test vs. each DMSO control, \*p<0.05).

**(E)** The block to infection is evident at the level of reverse transcription in IFN-treated THP-1.

**(F)** Treatment with the protein synthesis inhibitor cyclohexamide (CHX) rescues the IFN $\beta$ -induced block to LV.

**(G)** Known HIV-1 capsid mutations do not affect the IFN- $\beta$ -induced restriction in THP-1.

**(H)** THP-1 cells were pre-treated with 1ng/ml IFN $\beta$  for 24 h then transduced with VSV-g pseudotyped divergent retroviral vectors in the presence or absence of 5 $\mu$ M CsA.

**(I)** CB-derived CD34<sup>+</sup> cells were pre-stimulated with 1000 IU/mL of human IFN $\alpha$  for 24 hours followed by transduction with LV at an MOI of 1 in the presence or absence of 8 $\mu$ M CsH. Upregulation of selected IFN-stimulated genes (ISG) was assessed by RT-qPCR (mean  $\pm$  SEM, n=2).

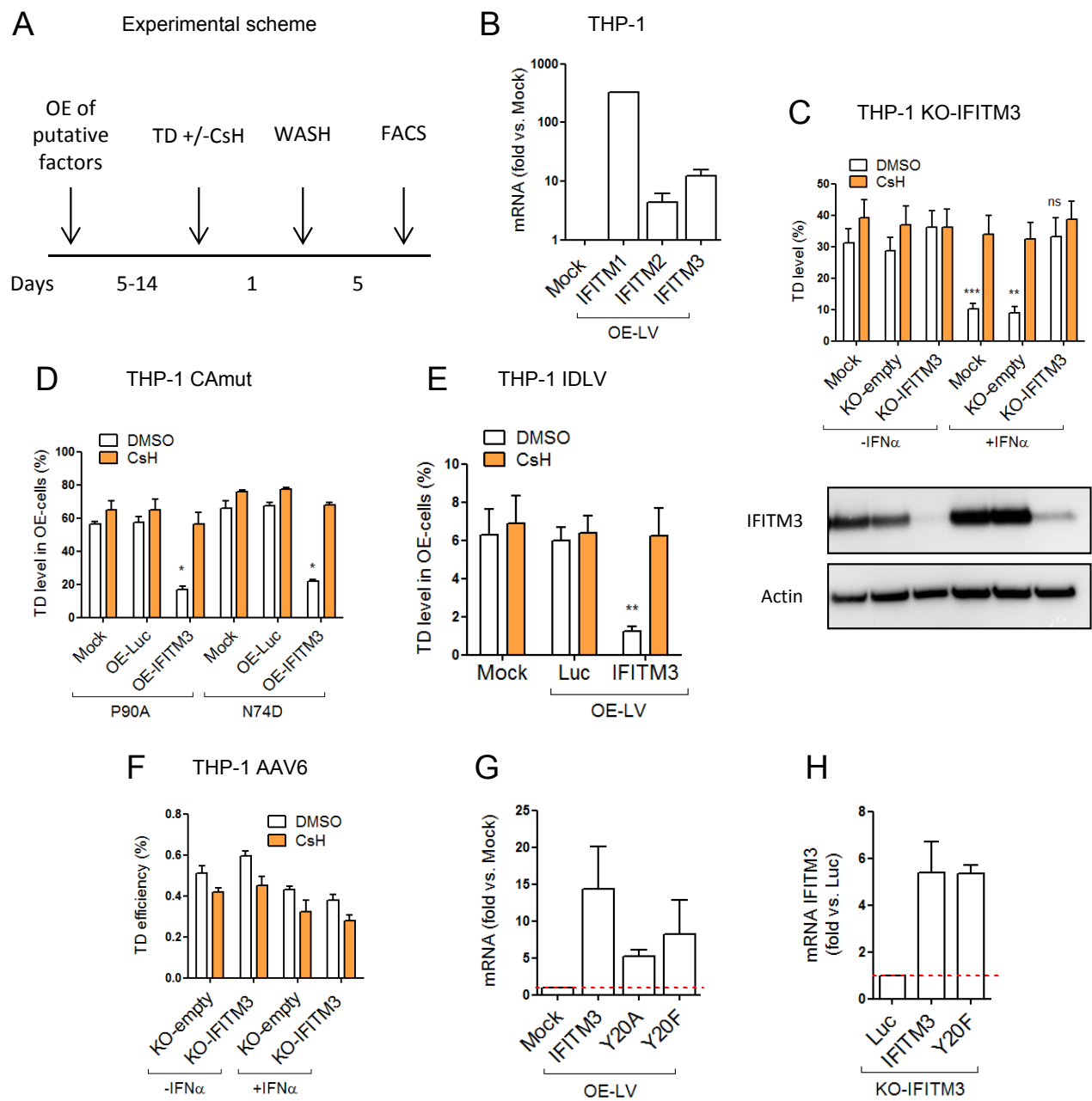


**Figure S4. CsA and CsH rescue IFITM3-dependent impairment of LV-TD in THP1 cell lines, Related to Figure 4.**

**(A)** Experimental scheme used in cell lines to see the impact of the over-expression (OE) of some candidate factors on transduction efficiency. THP-1 cells were transduced with an OE-LV and then re-challenged with a reporter LV at MOI 1 in the presence or absence of  $8\mu\text{M}$  CsH.

**(B)** mRNA levels were evaluated in THP-1 cells transduced with an LV expressing both GFP and IFITM or Luc (OE-LV) as in fig. 4A, B.

**(C)** THP-1 deleted for IFITM3 were re-challenged with a reporter LV at MOI 1 +/-  $8\mu\text{M}$  CsH. IFITM3 protein levels were evaluated at time of transduction (mean  $\pm$  SEM,  $n=10$ , Mann Whitney test vs. each control without  $\text{hIFN}\alpha$ , ns=not significant,  $**p\leq 0.01$ ,  $***p\leq 0.001$ ).

THP-1 cells over-expressing IFITM3 were transduced **(D)** with P90A or N74D capsid mutants (mean  $\pm$  SEM,  $n=4$ , Mann Whitney test vs. each control Luc,  $*p\leq 0.05$ ) or **(E)** an integrase-defective lentiviral vector (IDLV) (mean  $\pm$  SEM,  $n=6$ , Mann Whitney test vs. Luc,  $**p=0.0022$ ).

**(F)** THP-1 cells deleted for IFITM3 (KO-IFITM3) or control (KO-empty) were transduced with an AAV6 vector with or without CsH (mean  $\pm$  SEM,  $n=4$ ). Transduction efficiencies were assessed by FACS 3 days after the second transduction.

**(G, H)** mRNA levels were evaluated in THP-1 cells overexpressing the WT or mutated forms of IFITM3 as in fig. 4G, H (mean  $\pm$  SEM,  $n=3$ ).

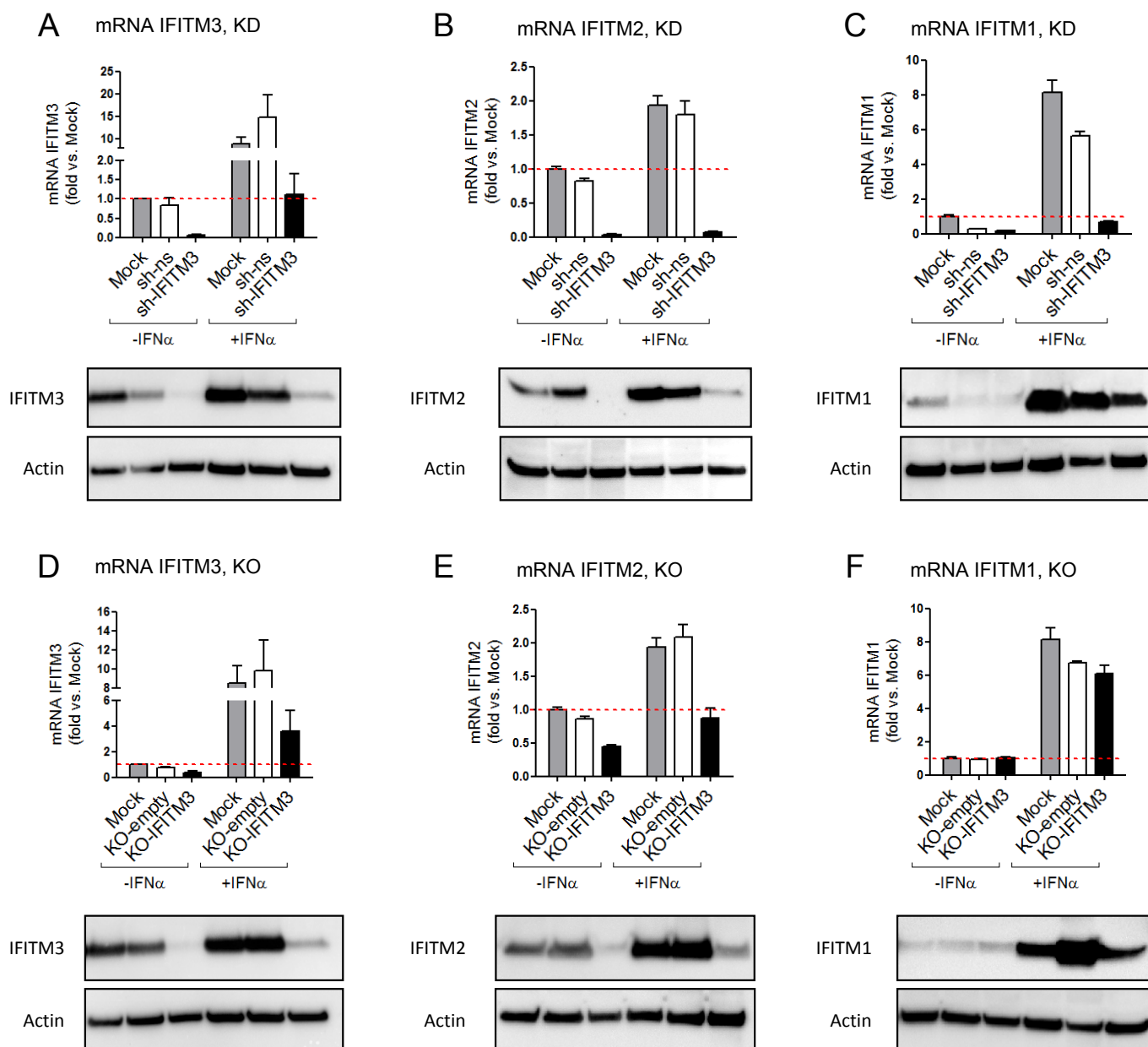
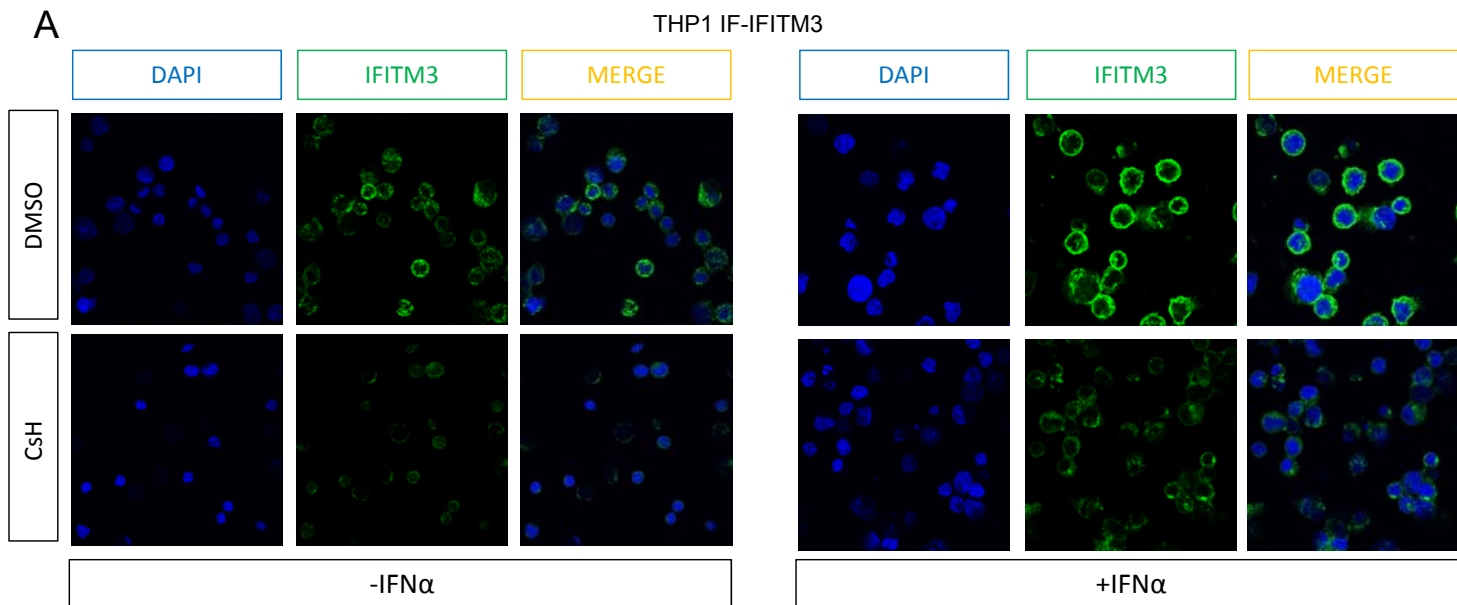


**Figure S5. IFITM3 KD/KO specificity in THP-1 cells, Related to Figure 4.**

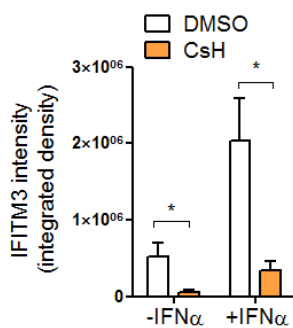
Levels of (A, D) IFITM3, (B, E) IFITM2 and (C, F) IFITM1 were measured by RT-qPCR and expressed as fold versus the Mock condition or by Western Blot in THP-1 cells depleted or deleted for IFITM3 as in Fig. 4C and S4C.



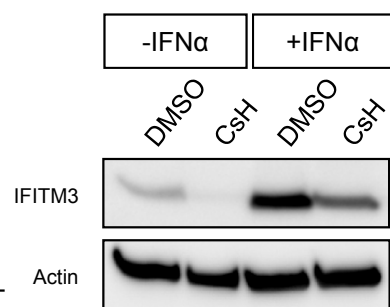
THP1 IF-IFITM3



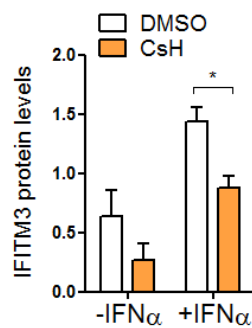
THP1 IF quantification



**B**

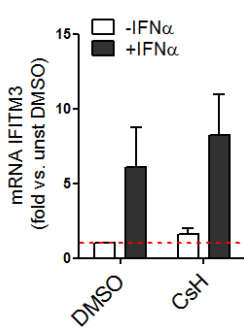


THP1 WB quantification

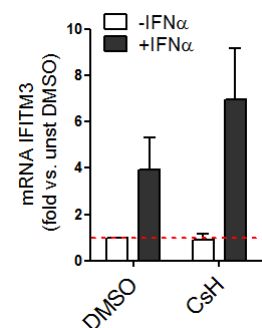


**C**

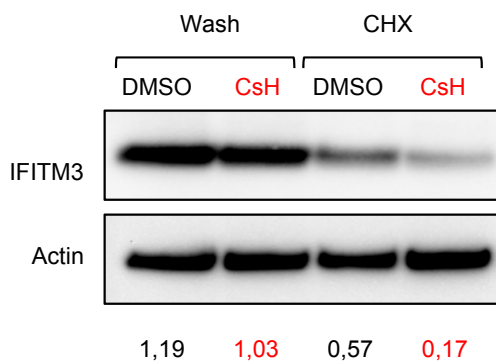
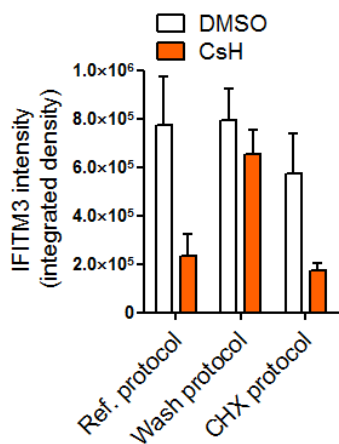
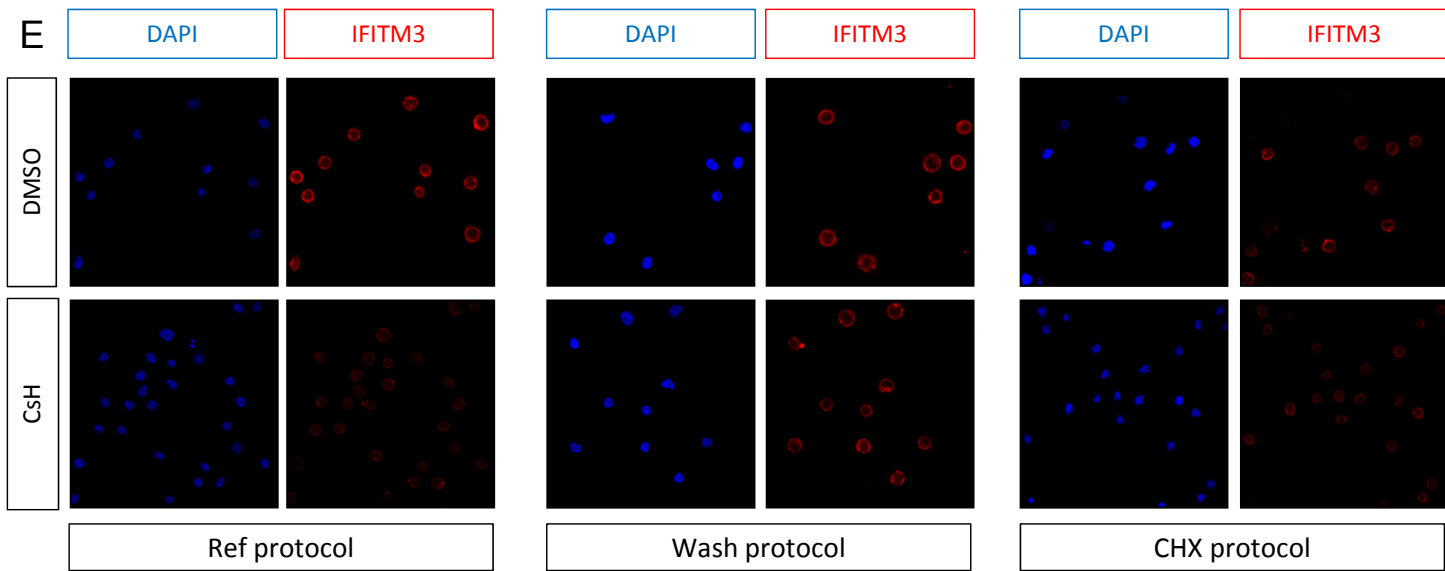
THP-1



**D** Human HSPC



**E**



**F**

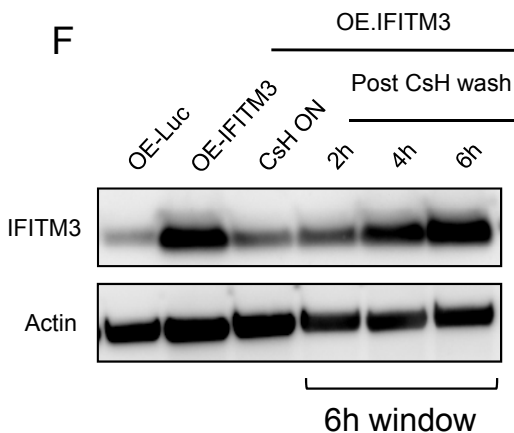


**Figure S6. CsH does not impact IFITM3 mRNA levels, Related to Figure 6.**

**(A-C)** THP-1 cells or **(D)** HSPC were pre-stimulated or not with 1000IU/mL IFN $\alpha$  for 24 hours followed by an over-night exposure or not to 8  $\mu$ M CsH.

IFITM3 protein levels were evaluated in THP-1 by **(A)** immunofluorescence (IF) using TCS SP5 Leica confocal microscope, 60x with oil and quantified as integrated density with ImageJ software (mean  $\pm$  SEM of three independent experiments in duplicate, n=15 images; Mann Whitney test versus DMSO, \*p $\leq$ 0.05) or by **(B)** Western Blot analysis and quantified by densitometry using ImageJ software using the Actin normalizer.

IFITM3 mRNA levels were measured in **(C)** THP-1 as well as in **(D)** HSPC by RT-qPCR and expressed as fold versus the DMSO control condition (mean  $\pm$  SEM, n=2-3).

**(E)** IFITM3 protein levels were evaluated in human CB-CD34<sup>+</sup> cells treated as in Fig. 3E by IF (mean  $\pm$  SEM of one representative experiment in duplicate, n=4 images) and WB (one representative blot out of two is shown) and quantified as previously described.

**(F)** IFITM3 protein levels were evaluated in THP-1 cells OE-IFITM3 at different time post CsH wash by Western Blot analysis (one representative blot out of two is shown).

**Table S1. List of oligonucleotides, Related to STAR Methods section.**

<b>Oligonucleotides</b>		
Human IFITM2 Fw primer GATGTCCACCGTGATCCAC	This paper	N/A
Human IFITM2 Rv primer GCAGCAGGTGTTTCATGAAG	This paper	N/A
Human IFITM3 Fw primer ATCACACTGTCCAAACCTT	This paper	N/A
Human IFITM3 Rv primer GTGCTCCTCCTTGAGCATCTC	This paper	N/A
LATE RT fw (DU3 sense) TCACTCCAACGAAGACAAGATC	<a href="#">(Petrillo et al., 2015)</a>	N/A
LATE RT rv (5NC2 rev) GAGTCCTGCGTCGAGAGAG	<a href="#">(Petrillo et al., 2015)</a>	N/A
2LTR fw (2junct) CAGTGTGAAAATCTCTAGCAGTAC	<a href="#">(Petrillo et al., 2015)</a>	N/A
2LTR rv (J2 rev) GCCGTGCGCGCTTCAGCAAGC	<a href="#">(Petrillo et al., 2015)</a>	N/A
Human Telo fw GGCACACGTGGCTTTTTCG	<a href="#">(Petrillo et al., 2015)</a>	N/A
Human Telo rev GGTGAACCTCGTAAGTTTATGCAA	<a href="#">(Petrillo et al., 2015)</a>	N/A
HIV sense TACTGACGCTCTCGCACC	<a href="#">(Petrillo et al., 2015)</a>	N/A
HIV antisense TCTCGACGCAGGACTCG	<a href="#">(Petrillo et al., 2015)</a>	N/A
HIV probe ATCTCTCTCCTTCTAGCCTC	<a href="#">(Petrillo et al., 2015)</a>	N/A
$\Delta$ U3 sense CGAGCTCAATAAAAGAGCCCAC	<a href="#">(Petrillo et al., 2015)</a>	N/A
PBS antisense GAGTCCTGCGTCGGAGAGAG	<a href="#">(Petrillo et al., 2015)</a>	N/A
sgRNA IFITM3 GGGGGCTGGCCACTGTTGACAGG	This paper	N/A
sgRNA AAVS1 TCACCAATCCTGTCCCTAGtgg	This paper	N/A
sgRNA IL2RG ACTGGCCATTACAATCATGTggg	This paper	N/A